Revista
Brasileira de
Ciência do Solo

Division – Soil in Space and Time | Commission – Soil Survey and Classification

Genesis and Classification of Soils Containing Carbonate on the Apodi Plateau, Brazil

Edilene Pereira Ferreira(1), Lúcia Helena Cunha dos Anjos(2), Marcos Gervasio Pereira(2)*, Gustavo Souza Valladares(3), Rafael Cipriano-Silva(4) and Antônio Carlos de Azevedo(4)

(1) Instituto Agronômico de Campinas, Programa de Pós-Graduação em Agricultura Tropical e Subtropical, Campinas, São Paulo, Brasil.
(2) Universidade Federal Rural do Rio de Janeiro, Departamento de Solos, Seropédica, Rio de Janeiro, Brasil.
(3) Universidade Federal do Piauí, Departamento de Geografia e História, *Campus* Ministro Petrônio Portella, Teresina, Piauí, Brasil.
(4) Universidade de São Paulo, Escola Superior de Agricultura “Luiz de Queiroz”, Departamento de Solos, Piracicaba, São Paulo, Brasil.

ABSTRACT: Information is scarce on the genesis and classification of soils derived from calcareous rocks in the Northeastern region of Brazil. This study describes the morphological, physical, chemical, mineralogical, and micromorphological properties of four soil profiles (P1-P4) located in the Apodi Plateau. A pedogenesis hypothesis and soil classification, according to the Brazilian System of Soil Classification (SiBCS), are proposed for these profiles. The interactions between parent material, surface topography and climate affected the pedogenesis processes and soil properties, although the calcareous nature of the parent material most affected the soil morphology and chemical properties. The sand fraction contained mainly quartz and calcite, and a smaller amount of mica. Smectite and interstratified illite-smectite occurred in the clay fraction of profile P1 and in some horizons of P2 (Ccmḱ and Ccrḱ) and P3 (2Ccrḱ). Kaolinite predominated in profiles P2, P3, and P4; where as illite and vermiculite were present in the Bicḱ, Bcḱ, Bcmḱ horizons of P2, in Bt2c of P3, and in C of P4. The mineralogy showed illite, hematite, and goethite, and anatase in a number of horizons. Micromorphological analysis of P2 indicated a strong cementation of Bcmḱ and Ccmḱ by calcium carbonate, and other properties indicate the formation of a petrocalcic horizon, but this horizon lacked lateral continuity in the profile. Therefore, the parapetrocalcic term is proposed for classifying P2 in the fourth level of the SiBCS. The 3Biḱ-P1 horizon exhibited calcite coating and iron coating or quasi-coating, indicating distinct pedogenesis processes occurring under different environmental conditions. Likewise, the occurrence of petroplinthite in P2 indicates that climatic conditions during its formation differed from present conditions, and both situations are interpreted as evidence that the soils were formed by polygenetic processes. In the SiBCS classification, the soils are classified as *Cambissolo Háplico Carbonático vertissólico* (P1), *Cambissolo Háplico Carbonático concrecionário* (P2), *Luvissolo Crômico Pálico petroplíntico* (P3), and *Neossolo Litólico Carbonatico típico* (P4); and a new class (*parapetrocálcico concrecionário*) is proposed for P2 in the fourth level.

Keywords: Karst system, Brazilian Soil Classification System, soil mineralogy, soil micromorphology.

*** Corresponding author:**
E-mail: gervasio@ufrrj.br

Received: January 23, 2015

Approved: October 10, 2015

How to cite: Ferreira EP, Anjos LHC, Pereira MG, Valladares GS, Cipriano-Silva R, Azevedo AC. Genesis and Classification of Soils Containing Carbonate on the Apodi Plateau, Brazil. Rev Bras Cienc Solo. 2016;v40:e0150036.

DOI: 10.1590/18069657rbcs20150036

INTRODUCTION

Among the soils developed in the karstic landscape of Northeastern Brazil, those from the Apodi Plateau (Jandaíra formation), which extends from the state of Ceará to Rio Grande do Norte, are distinguished by their contrasting characteristics and intense agricultural use. Nevertheless, information on their pedology is scarce. In the Apodi Plateau, the compactness of the calcareous parent material may limit local drainage, while subsurface fractures favor hydrologic flux in the landscape as a whole. The mineralogical composition of the limestone is also variable, changing the pattern according to the accessory minerals. In addition to these conditions, the regional climate and relief features have a strong influence on soil formation (Silva et al., 2013).

The most common soils developed from limestone in Brazil are equivalent to Mollisols, Vertisols, vertic and/or carbonatic Inceptisols, and some Alfisols and Ultisols (Shinzato, 1998). Some studies on soil genesis in the Brazilian karstic landscape were done by Ernesto Sobrinho (1979), Alencar (2002), Lynch (2009), Girão (2013), Pereira et al. (2013), and Silva et al. (2013). According to the Brazilian Soil Classification System – SiBCS (Santos et al., 2013), the main diagnostic feature in soils on karstic landscapes are carbonate or hypocarbonate properties, and calcic and petrocalcic diagnostic horizons. In these horizons, carbonate accumulation influences chemical characteristics such as pH, soil buffering, cation exchange capacity (CEC), and nutrient availability to plants (Moreira et al., 2000; Khresat, 2001). In addition, morphological characteristics such as continuous cementation may occur as the process of calcification advances.

This study was motivated by scarcity of information on characteristics of soils with horizons rich in carbonate, particularly in tropical environments. The objective was to characterize the morphological, physical, chemical, mineralogical, and micromorphological properties of soils derived from calcareous rocks in the Apodi Plateau, in the Northeastern region of Brazil. An additional objective was to propose a theory based on these properties to explain the genesis of the soils and to classify the soils according to the SiBCS.

MATERIALS AND METHODS

The study was carried out on the Apodi Plateau in the Northeastern region of Brazil. The climate in the region is BSw'h' (very hot and semi-arid), according to the Köppen classification. Mean rainfall is 750 mm yr^{-1}, concentrated from February to May, and the evapotranspiration reaches 3,215 mm yr^{-1} (Brasil, 1973; Fernandes et al., 2005), resulting in a high water stress. The topography is a predominantly flat plateau, with small areas of gently rolling hills. Parent material is calcareous rock from the Jandaira Formation, Apodi Group. Bioclastic lime, sandstone-lime, and dolomitic limestone are the most common components; the first two rocks are light gray, white, or yellow in color, with fine to medium texture, and the dolomitic limestone is gray or yellow and frequently have coarser texture (Brasil, 1981).

Four soil pits were dug for description and sampling of the profiles (P1, P2, P3, and P4) in May 2010 (Figure 1). The profiles were located along a transect representative of landscape vegetation and relief in the Apodi Plateau. The geographic coordinates are 5° 9' 31.62" S, 38° 02' 53.26" W for P1; 5° 03' 22.42" S, 37° 38' 57.37" W for P2; 5° 07' 23.75" S, 37° 56' 34.91" W for P3; and 5° 09' 05.87" S, 38° 02' 12.99" W for P4; the transect extended for nearly 50.4 km. Samples were taken from all the horizons for chemical, physical, and mineralogical analysis, and bulk undisturbed samples were collected from the P1-3Biḱ and P2-Bicḱ horizons for micromorphological analysis (Santos et al., 2005).

Chemical and physical analyses of air-dried fine earth samples were performed according to Claessen (1997). Particle size was assessed using sodium hexametaphosphate as a dispersant. Soil pH (water, KCl, and $CaCl_2$, 1:2.5) and the exchangeable complex (Ca^{2+}, Mg^{2+}, K^+, Na^+, H^+ and Al^{3+}) were also determined. The $CaCO_3$ equivalent was measured using 0.5 mol L^{-1} HCl, titrated with NaOH. Phosphorus was measured according to Claessen (1997) using calcium bicarbonate solution (Olsen et al., 1954).

Mineralogical analysis of sand, silt, and clay fractions were performed by X ray diffraction (XRD), with random powder mounts of the sand and silt specimens. The clay specimens were analyzed in their natural condition and after the following treatments: extraction of Fe oxides with citrate-dithionite-bicarbonate (CDB), as described by Mehra and Jackson (1960); saturation with K, mounted on a slide and read at 25 °C and, after heating for 2 h, at temperatures of 350 and 550 °C; saturation with Mg and a reading at 25 °C before ethylene glycol solvation. The clay specimens were mounted on oriented slides. A Rigaku Miniflex device equipped with a graphite-monochromated Cu Kα radiation source (30 kV, 15 mA) was used for mineralogy analyses. The samples were scanned using a step size of $0.050° s^{-1}$, in a 2θ range of 2° to 45°.

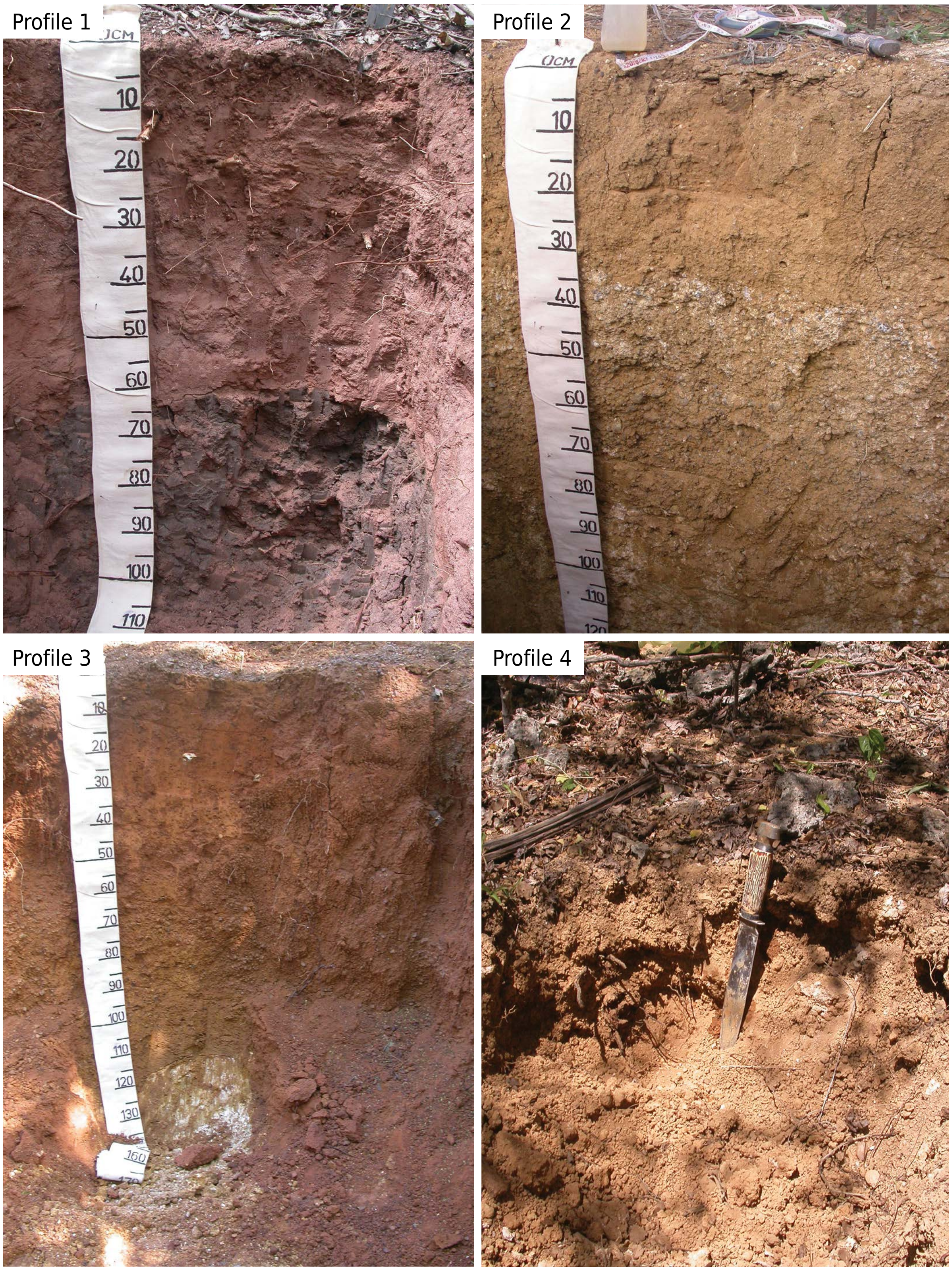

Figure 1. Soil profiles sampled on the Apodi Plateau (Photos by Ricardo Espíndola).

Undisturbed samples were dried at room temperature for 20 days and in a laboratory oven at 35 °C for 7 days. After that, samples were impregnated with polyester resin, styrene monomer, and fluorescent pigment, using Butanox as polymerization catalyst (Castro et al., 2003). Sections with maximum thickness of 30 µm were analyzed under a Zeiss petrographic microscope with both normal and polarized light. Thin sections were described according to Stoops (2003) and Bullock et al. (1985).

RESULTS AND DISCUSSION

Profile P1 is somewhat poorly drained and is located at the footslope; the area has gently rolling relief and 39 m of elevation. Profiles P2 and P3 are at the top of the plateau, with plain topography (0-1 % and 2 % slope, and 97 and 141 m elevation, for P2 and P3, respectively) and they are moderately well drained. The parent material of P2 and P3 is reworked sediments from calcareous rocks. Profile P4, located on a backslope, at 97 m elevation, is well drained and formed from calcareous rocks. The profile position in the landscape is an important factor for pedogenesis. For instance, in a study in India, Shankar and Achyuthan (2007) observed laminar petrocalcic horizons on the plains and calcic horizons on the slopes of the study area.

Morphological properties

Profile P1 had a hue from 5YR to 2.5YR and value and chroma of 3 or 4 (Table 1). Exceptions were the 3Biḱ horizon, due to the pink color of calcite grains (5YR 7/4), and the 5Bvk horizon, with 5Y 5/1 and mottles of 5YR 6/8. P1 exhibited a silt loam texture, except for the 5Bvk horizon, which showed a clay loam texture and friction surfaces. The morphological characteristics of the profile, along with micromorphological observations and carbonate content, suggest sediment stratification and deposition (Silva et al., 2013), which was therefore characterized as lithological discontinuity. Color in P2 was 10YR, value 4 and chroma from 3 to 6, and became variegated below 0.51 m due to the increase in carbonate content. Soil in P1 exhibited a variation of texture and the presence of nodules (petroplinthite and other types), in addition to shell fragments in the sand, gravel, and cobble fractions, from the Ap1 to Bḱ horizon. Petroplinthite was found in more than 50 % of the volume of the Ccmḱ horizon, in the gravel and cobble fractions, and color was variegated, with dark yellowish brown (10YR 4/4, 10YR 4/6) and dark reddish brown (2.5YR 3/4). Iron and Mn concretions were reported in the Baixio do Irece (state of Bahia) and in the north of the state of Minas Gerais (Alencar, 2002), at increasing amounts with depth.

Like P2, profiles P3 and P4 exhibited shell fragments. Profile P3 had a hue of 5YR, but chroma and value changed with depth. The colors suggest slower water permeability in the profile below 0.63 m, possibly influenced by the prismatic structure, clayey texture, and proximity to rock in the 2Ccrḱ. The *solum* (A and B horizons) was shallow, and the BC and 2Ccrḱ horizons were very hard to extremely hard when dry. In addition to low soil permeability, regional climate changes between the dry and wet periods result in a seasonal redox variation, favoring the formation of ferromanganese concretions and petroplinthite (Schwertmann and Taylor, 1989). Profile P4 had a shallow depth, with an ACR sequence and high gravel and rock fragment content. The rolling topography and the slope position decrease water infiltration, increasing surface flow and soil losses.

The color variations observed in the profiles are common in calcareous soils. The reddish color is related to a climate with a short rainy season and high evapotranspiration. During the dry season, the Fe released from parent material through weathering reactions precipitates and gives rise to pedogenic hematite after dehydration and rearrangement of less crystalline forms (ferrihydrite) (Schwertmann and Taylor, 1989; Yaalon, 1997). In profiles P2 and P4, however, the yellowish color reveals the presence of goethite.

The most remarkable morphological feature in P2 was the precipitation of secondary carbonate, which was confirmed by $CaCO_3$ equivalent values in the subsurface horizons (Table 2). The thickness of the Bcmḱ horizon (0.51 to 0.70 m) was greater than 0.10 m, and its consistency ranged from extremely hard to extremely firm. The consistency of the Bcḱ horizon (0.70 to 0.79 m) was very hard and friable, and the horizon contained mottles formed by calcium carbonate. In the Ccmḱ horizon (0.79 to 0.86 m), gravel-sized concretions were extremely hard, and the remaining material was loose, while soil consistency was extremely firm. The Bcmḱ and Ccmḱ horizons exhibited strong Ca carbonate cementation, and their morphology met most requirements for petrocalcic horizons, except for the lack of lateral continuity. In P2, petroplinthite (the "c" suffix of Ccḱ and Ccmḱ) possibly affected water percolation and favored carbonate accumulation and cementation in the subsurface. However, in spite of the water deficit in this semi-arid region, the rainfall on the Apodi Plateau likely led to carbonate dissolution.

Table 1. Morphological properties of soils from the Apodi Plateau

Hor(1)	Depth	Color (wet soil) Matrix	Structure(3)	Consistency(4)			Trans(5)	Texture(6)
				Dry	Moist	Wet		
	m		Profile P1					
Aḱ	0.00–0.03	5YR 4/3	st, me, sab/st, vf,gr	VH	VFi	SPL/SST	sm/clr	si–l
Abḱ	0.03–0.11	5YR 4/3	mo, f/me, sab	H	Fr	SPL/ST	sm/clr	si–l
2Biḱ	0.11–0.20	5YR 4/4	wk, me/f, sab	S	VFr	SPL/SST	sm/ abp	si–l
3Biḱ	0.20–0.31	2.5YR 3/4	wk, me, pr/sab	S	VFr	SPL/SST	sm/ abp	si–l
4Bcḱ	0.31–0.56	2.5YR 4/4	wk, f, sg/gr	S	VFr	SPL/SST	sm/ abp	si–l
5Bvk	0.56–0.95+	5Y 5/1(2)5YR 6/8	st, vco, pr *porst, co, pr	EH	Efi	VPL/ST	–	cl–l
			Profile P2					
Ap1	0.00–0.03	10YR 4/3	st, me, l	VH	Fr	VPL/ MST	sm/clr	cl–l
Ap2	0.03–0.19	10YR 4/4	ma	H	Fr	VPL/ MST	sm/ clr	cl
Biḱ	0.19–0.32	2.5Y 4/4	mo, f/me, sab/pr	SH	F	PL /ST	sm/ clr	cl–si
Bicḱ	0.32–0.51	10YR 4/6	mo/wk, f, sab	S	VFr	PL /ST/SST	wav/abp	cl–l–gr
Bcmḱ	0.51–0.70	Variegated	ma	EH	Efi	NPL/NST	sm/clr	cl–l–gr
Bcḱ	0.70–0.79	10YR 5/4,(2) 5Y 8/1	st, f/me, ab	VH	Fr	PL /ST	sm/clr	cl
Ccmḱ	0.79–0.86	Variegated	sg	*	Efi	NPL/NST	sm/dis	l–gr
Ccḱ	0.86–1.02	2.5Y 5/6	ma	SH	Fr	PL /ST	dis/ abp	si–l
Ccrk	1.02–1.33+	Variegated	ma	S	Fr	PL /SST/ST	–	si
			Profile P3					
Ac	0.00–0.05	5YR 3/3	mo, sg/f, sab	S	VFr	NPL /SST	sm/abp	l–gr
Bac	0.05–0.10	5YR 4/4	st, f, sab	S	VFr	PL /ST	sm/clr	cl–l
Bt1c	0.10–0.39	5YR 5/8	mo, f, pr	SH	VFr	VPL/ST	sm/dis	cl
Bt2c	0.39–0.63	5YR 6/8	mo, f/vf, pr/sab	SH	VFr	VPL/ST	sm/dis	cl
Bt3c	0.63–0.88	7.5YR 5/8	mo,f/vf, sg/pr	SH	VFr	PL /ST	sm/abp	cl
2BCc	0.88–1.08 (1.06–1.18)	10YR 5/8	mo, me/co, ab	EH	Fi	VPL/ MST	–	cl
2Crkc	1.08–1.30+	Variegated	ma	VH	Fi	PL /ST	–	si–l
			Profile P4					
A	0.00–0.10	10YR 3/4	wk, f, gr/mo,f, sab	L	L	NPL /SST	–	l–gr
C	0.10–0.27	7.5YR 4/6	sg	L	L	NPL /SST	–	l–gr
R	–	–	–		–			–

(1) Horizon (Hor). (2) Variegated. (3) Structure: weak (wk), moderate (mo), strong (st), very fine (vf), fine (f), medium (me), coarse (co), very coarse (vco); angular blocky (ab), subangular blocky (sab), massive (ma), granular (gr), single grain (sg), platy (l), prismatic (pr). (4) Consistency: loose (L), soft (S), slightly hard (SH), hard (H), very hard (VH), extremely hard (EH); very friable (VFr), friable (Fr), firm (Fi), very firm (VFi), extremely firm (EFi); plastic (PL), slightly plastic (SPL),very plastic (VPL); slightly sticky (SST), sticky (ST), non-plastic (NPL), non-sticky (NST). (5) Transition (Trans): smooth (sm), wavy (wav); abrupt (abp), clear (clr), gradual (grd), and discontinuous (dis). (6) Texture: silt loam (si-l), clay loam (cl-l), clay (cl), silty clay (si-cl), clay loam with gravel (cl-l-gr), loam with gravel (l-gr). In the Brazilian norms for soil description, the i horizon suffix is equivalent to the w in the Field Book for Describing and Sampling Soils (USDA/NRCS/NSSC).

Physical properties

The profiles contained a large amount of gravel, cobbles, and silt (Table 3). In P2 and P3, some of the particles larger than 2 mm were petroplinthite with irregular distribution, and in P2 the plinthite content was significantly higher, accounting for more than 50 % of the fine earth fraction in the Ccḱ and Ccmḱ horizons. In P3, petroplinthite levels were lower and scattered throughout the horizons. In a similar condition in the state of Minas Gerais, it was suggested that the occurrence of ferromanganese concretions associated with $CaCO_3$ was evidence of the current dry climate (Oliveira et al., 2001).

In young soils formed from sedimentary parent material, the silt/clay ratio depends on the particle size of the material deposited. In P1, the heterogeneity of this ratio suggests lithology discontinuity, probably caused by sediments deposited on the footslope where this profile is located. Such sediments are produced by reworked material from the Jandaira Formation. The calcareous nature of P1 is indicated by the high carbonate content (Table 3) and pedological features such as calcite coatings and fillings (Table 4). By contrast, the silt/clay ratio in P2 and P4 was inherited from the limestone.

Table 2. Calcium carbonate ($CaCO_3$) equivalent, organic carbon level, pH, chemical properties, and phosphorus of soils from the Apodi Plateau

Hor[1]	$CaCO_3$ equiv.	TOC[2]	pH[3]			ΔpH[4]	Exchangeable complex									P	
			H_2O	KCl	$CaCl_2$		Ca^{2+}	Mg^{2+}	Ca/Mg	K^+	Na^+	SB	H^+	T	V	Melich-1	Olsen
	g kg^{-1}						cmol$_c$ kg^{-1}			cmol$_c$ kg^{-1}					%	mg kg^{-1}	
								Profile P1									
Aḱ	104.5	10.9	8.6	7.2	7.7	-1.4	25.6	3.3	8	0.59	0.47	30.0	0.0	30.0	100	24	3
ABḱ	122.7	6.9	8.6	7.3	7.7	-1.4	24.4	2.7	9	0.26	0.15	27.5	0.0	27.5	100	23	1
2Biḱ	94.5	2.8	8.9	7.5	7.7	-1.5	14.0	5.1	3	0.18	0.11	19.4	0.0	19.4	100	19	1
3Biḱ	108.2	2.2	8.7	7.1	7.7	-1.6	22.1	4.1	5	0.15	0.10	26.5	0.0	26.5	100	25	1
4Bcḱ	76.4	2.2	8.9	7.4	7.7	-1.6	17.7	3.1	6	0.13	0.13	21.1	0.0	21.1	100	23	1
5Bvk	9.1	1.9	8.7	7.1	7.7	-1.6	20.8	7.5	3	0.21	0.68	29.2	0.0	29.2	100	6	2
								Profile P2									
Ap1	200.0	13.1	8.3	7.8	7.9	-0.5	11.2	3.2	4	0.63	0.61	15.6	0.0	15.6	100	6	4
Ap2	163.6	9.1	8.4	7.5	7.7	-1.0	13.6	2.3	6	0.17	0.28	16.4	0.0	16.4	100	4	3
Biḱ	254.6	6.4	8.5	7.6	7.7	-0.9	12.4	2.4	5	0.08	0.30	15.2	0.0	15.2	100	3	2
Bicḱ	290.9	2.0	8.6	7.8	7.8	-0.8	8.0	1.5	5	0.04	0.34	9.9	0.0	9.9	100	3	2
Bcmḱ	232.7	3.7	8.5	7.5	7.7	-1.0	10.6	1.5	7	0.04	0.24	12.4	0.0	12.4	100	3	2
Bcḱ	305.5	3.4	8.4	7.5	7.7	-0.9	13.6	1.5	9	0.03	0.21	15.3	0.0	15.3	100	3	1
Ccmḱ	652.7	2.4	8.5	7.7	7.8	-0.8	11.3	1.6	7	0.03	0.13	13.1	0.0	13.1	100	3	1
Ccḱ	794.6	1.8	8.5	7.7	7.8	-0.8	7.1	0.9	8	0.03	0.16	8.2	0.0	8.2	100	3	2
Ccrk	849.1	1.2	8.9	8.2	7.8	-0.7	4.7	1.1	4	0.03	0.16	6.0	0.0	–	–	–	–
								Profile P3									
Ac	0.0	12.2	7.8	6.6	6.8	-1.2	6.7	3.3	2	0.74	0.06	10.8	0.7	11.5	94	5	3
BAc	0.0	7.0	7.4	5.9	6.3	-1.4	7.3	3.2	2	0.95	0.10	11.5	0.7	11.9	95	3	2
Bt1c	0.0	5.2	7.5	5.6	6.2	-1.9	9.0	3.1	3	0.34	0.09	12.5	1.7	13.5	92	4	3
Bt2c	0.0	3.1	7.5	5.9	6.7	-1.6	9.8	3.0	3	0.20	0.14	13.1	1.0	14.0	93	3	2
Bt3c	0.0	2.2	7.6	6.2	7.1	-1.4	9.7	2.8	3	0.10	0.09	12.7	0.7	13.0	95	3	2
2BCc	0.0	1.9	8.1	6.4	7.1	-1.8	17.3	2.6	7	0.10	0.06	20.0	0.0	20.0	100	3	2
2Crkc	544.0	1.5	8.7	7.6	7.7	-1.1	11.0	2.2	5	0.05	0.09	13.3	0.0	13.3	100	3	2
								Profile P4									
A	325.0	23.3	8.4	7.5	7.6	-0.9	15.0	1.4	11	0.23	0.30	16.9	0.0	16.9	100	110	18
C	472.0	20.6	8.3	7.5	7.5	-0.8	13.4	0.9	15	0.10	0.10	14.5	0.0	14.5	100	81	19
R	–	–	––	–	–	–	–	–	–	–	–	–	–	–	–	–	–

[1] Hor: Horizon. [2] pH (soil:solution 1:2.5). [3] TOC: total organic carbon. [4] Delta (Δ) pH = pH(KCl) – pH(H_2O). S: sum of bases (SB = Ca^{2+}+Mg^{2+}+K^++Na^+); T: cation exchange capacity at pH 7.0 (CEC = S + H+Al); V: base saturation (V = 100 S/T).

Table 3. Particle size, flocculation degree, silt/clay ratio, and coarse sand/fine sand ratio of soils from the Apodi Plateau

Hor(1)	Depth	Particle Size							FD(3)	Silt/ Clay	CS/FS(4)
		Cobble	Gravel	ADFE(2)	Sand		Silt	Total clay			
					AG	AF					
	m	g kg^{-1}							%		
		Profile P1									
Aḱ	0.00–0.03	0	3	997	219	18	567	196	100	2.90	12.2
ABḱ	0.03–0.11	0	9	991	248	22	559	171	100	3.27	11.2
2Biḱ	0.11–0.20	0	10	990	348	37	501	115	100	4.38	9.4
3Biḱ	0.20–0.31	0	8	992	255	27	606	113	100	5.39	9.6
4Bcḱ	0.31–0.56	0	6	994	309	33	570	89	100	6.44	9.4
5Bvk	0.56–0.95+	0	26	974	246	22	356	377	100	0.95	11.1
		Profile P2									
Ap1	0.00–0.03	156	0	844	204	9	374	414	100	0.90	22.5
Ap2	0.03–0.19	58	0	942	177	10	352	461	100	0.77	17.7
Biḱ	0.19–0.32	34	0	966	132	9	436	424	100	1.03	15.5
Bicḱ	0.32–0.51	539	106	355	356	8	360	276	100	1.30	42.1
Bcmḱ	0.51–0.70	548	97	355	261	7	359	373	100	0.96	39.0
Bcḱ	0.70–0.79	326	30	643	116	7	393	485	100	0.81	17.7
Ccmḱ	0.79–0.86	179	630	191	421	5	468	106	100	4.42	84.2
Ccḱ	0.86–1.02	124	0	876	82	3	762	154	100	4.96	27.2
Ccrk	1.02–1.33+	48	0	952	33	2	863	101	100	8.50	14.7
		Profile P3									
Ac	0.00–0.05	344	0	656	284	32	441	244	100	1.81	8.9
BAc	0.05–0.10	69	0	931	177	31	396	397	100	1.00	5.7
Bt1c	0.10–0.39	83	0	917	152	25	367	457	100	0.80	6.1
Bt2c	0.39–0.63	200	0	800	170	23	316	491	100	0.64	7.3
Bt3c	0.63–0.88	330	5	665	191	14	341	454	100	0.75	13.3
2BCc	0.88–1.08 (1.06–1.18)	487	0	513	85	23	370	522	100	0.71	3.7
2Crkc	1.08–1.30+	355	0	645	142	37	617	204	100	3.03	3.9
		Profile P4									
A	0.00–0.10	315	122	563	346	17	450	187	100	2.42	20.2
C	0.10–0.27 (0.24–0.27)	312	166	522	400	16	381	204	100	1.87	24.6
R	–	–	–	–	–	–	–	–	–	–	–

(1) Hor: Horizon. (2) ADFE: air-dried fine earth. (3) DF: flocculation degree. (4) CS/FS: coarse sand/fine sand.

The high Ca levels accumulated as carbonates in P1 and P2 increased clay flocculation, reaching values of 100 % in all the profiles. In P3, clay levels increased with depth despite clay flocculation and accumulation in the Bt horizon. Clay translocation may occur through water flowing preferentially along macropores when the volume of infiltrated water is high (Holliday, 1985). In the semi-arid region, this should take place during the rainy season, when rainfall is intense.

Chemical properties

Soil pH ranged from 7.4 to 8.9 in water, 5.6 to 8.2 in KCl solution, and 6.2 to 7.9 in $CaCl_2$ solution (Table 2). Delta-pH was negative in all the horizons, indicating predominance of net negative charge on the surface of soil particles. Calcareous soils from Iran showed pH (H_2O) ranging from 7.1 to 8.2 (Khormali et al., 2003), and nearly 7 (in water) and 6.5 (in KCl solution) in Spain (Taboada Castro and Silva Hermo, 1999). Khresat and Taimeh (1998) described an increase in pH with depth and in carbonate content in Vertisols from Jordan.

Potassium contents in surface horizons were very high in P1, P2, and P3 and moderate in P4, and they decreased in the subsurface in all the profiles. Higher K contents in farming areas arise not only from fertilizer application but also because mica presence and higher K release due to parent materials, which are rich in Ca and Mg. An increase in K contents in the surface soil due to the presence of mica was also observed by Khresat and Taimeh (1998) in Vertisols from semi-arid areas in Jordan.

The soil profiles exhibited high sum of bases (SB) and T values (CEC) because of the significant contribution of Ca ions, which ranged from 4.7 to 25.6 $cmol_c$ kg^{-1}. The high Ca/Mg ratio, however, causes nutritional imbalance in plant physiology. Base saturation (V) was high in all the profiles, and Al concentration was zero.

Phosphorus concentration (Table 2) was higher when determined by Mehlich-1 than the Olsen method, particularly in P1 and P4. It is noteworthy; however, that in calcareous soils the Mehlich-1 extractor possibly overestimates available P because the low pH of the solution may dissolve P sources that are not available to plants, such as Ca phosphate (P-Ca) (Lemos et al., 1997). In contrast, the pH value of the extracting solution used by the Olsen method is buffered in the alkaline range, matching the pH of calcareous soils and extracting only available forms. Based on the Olsen P results, P concentration in most horizons was low (from 1.0 to 3.0 mg kg^{-1} in P1, P2, and P3) and moderate in P4 (from 18 to 19 mg kg^{-1}). High total P content is commonly reported in calcareous soils due to the presence of low-solubility Ca phosphate (Pansu and Gautheyrou, 2006), but the content of available P may be very small.

Table 4. Micromorphological description of selected horizons in soil profiles P1 and P2 from the Apodi Plateau

Overall	Coarse material	Fine material	Microstructure	Pores	Pedological features
ProfileP1 – 3Biḱ (0.20-0.31 m)					
One zone	15 % groundmass, well selected and containing quartz (50 %), feldspars (20 %), calcite (10 %), and other (10 %). Smooth, sub-spherical and sub-angular (60 %), smooth, sub-angular and sub-elongated (40 %). Irregular alteration.	50 % groundmass, dark brownish yellow, composed of clays, iron oxides, and calcium carbonate. Crystallites: Cross-striated (10 %), granostriated and porostriated (60 %), mottled (30 %).	Type: complex microstructure; sub-angular blocky peds: 70 % mildly developed, not accommodated, and granular; 30% well developed, not accommodated. Porphyric distribution.	35 % groundmass, with chambers (60 %), channels (20 %), cavities and fissures (20 %). Irregular wavy surface.	Micrite coating and dense incomplete micrite infilling; typical pure (80 %), composed (15 %), calcite nodules and concentric nodules (5 %). Typical Fe and clay coating and hypo-coating. Pore filling with adherent loose material (continuous and discontinuous). Typical nodules, pure and strongly impregnated with Fe, Mn, organic matter, and clay (15 %). Dense and intact spherical/ellipsoidal excrements. Loose, discontinuous infilling.
Profile P2 – Bicḱ (0.32-0.51 m)					
One zone	20 % groundmass, mildly selected and containing quartz (50 %), feldspars (15 %), calcite (20 %), and other (5 %). Smooth, sub-spherical, sub-rounded (45 %), smooth, sub-spherical, sub-elongated (45 %), smooth, sub-elongated, and sub-rounded (10 %). Without alteration and with irregular alteration	60 % groundmass, dark brownish yellow, composed of clays, iron oxides and calcium carbonate. Crystallites: granostriated and porostriated (40 %), mottled and mosaic (60 %)	Type: complex microstructure. Sub-angular and angular blocky peds: 80 % mildly developed, partially accommodated, and granular; 20 % well developed, not accommodated. Porphyric distribution.	20 % groundmass, with chambers (50 %), cavities and fissures (40 %), channels (10 %). Irregular wavy surface.	Micrite coating and dense incomplete and loose discontinuous micrite infilling; calcic nodules (90 % pure or impregnative, 10 % composed and concentric). Pore filling with adherent loose material (continuous and discontinuous). Typical nucleic and porous nodules strongly impregnated with Fe, Mn, organic matter, and clay (15 %).

Calcium carbonate ($CaCO_3$) equivalent, a method to determine carbonate content in calcareous materials or soils, simulates a situation where $CaCO_3$ is the only carbonate in the soil. In the soils under study, the $CaCO_3$ equivalent values ranged from 9.1 to 849.1 g kg^{-1} (Table 2), and in most horizons from P2 and P4, these values were higher than the limit defining calcic horizons according to the SiBCS (Santos et al., 2013). Calcite accumulation was observed in most horizons, which is in agreement with the high $CaCO_3$ content observed.

Carbonate distribution and calcite accumulation in P1 and P2 was irregular. This distribution is related to the pedogenic carbonate formation (Dal'Bó and Basilici, 2010), and in the future, this feature may be used as a criterion to differentiate carbonate accumulation by pedogenic processes from carbonate accumulation by deposition due to sedimentation or parent material stratification. In P1, these values decrease with depth, possibly because the profile position (footslope) favors the accumulation of ions leached from more elevated positions on the slope (Silva et al., 2013). In profile P3, most of the horizons did not exhibit values of $CaCO_3$ detectable by titration in the laboratory, except in the horizon lying over the limestone (544.0 g kg^{-1} $CaCO_3$ equivalent in P3-2Crḱ). In contrast, P4 showed high $CaCO_3$ content, as a contribution from the underlying parent material, given that carbonate values increased with depth.

Since P3 is located on a homogeneous flat plain, the lack of carbonate in the *solum* may be due to micro relief. In another study on Apodi Plateau soils, in areas of low relief near the profiles sampled in this study, Oliveira et al. (2013) found wide variation in soil properties, such as greater clay content and deep profiles in concave form surfaces, suggesting that pedogenesis was higher because of convergent water flow. In addition, P3 is located above P2, where accumulation and cementation by $CaCO_3$ was observed. In a study on polygenetic soils, Chadwick et al. (1995) observed changes in soil properties, such as carbonate loss and decrease in pH (<7.0), accompanying the increase in profile depth along the transect.

Calcium carbonate accumulation in the profile and the genesis of calcic and petrocalcic horizons start with the translocation of soluble bicarbonates in the soil solution and their precipitation, processes that depend on climate, as well as soil relief and stability where the soils are formed (Bachman and Machette, 1977). Secondary carbonate concretions and nodules are common in Vertisols from calcareous rocks, usually in landscape positions that favor the buildup of Ca and Mg ions in the soil solution (Hendricks, 1991). In addition, *in situ* alterations of primary $CaCO_3$ by dissolution, translocation, and further precipitation form secondary $CaCO_3$ concretions, mainly in the form of calcite (Rabenhorst et al., 1991). The dissolution/precipitation of calcite is affected by several factors, including pH, partial CO_2 pressure, temperature, and water loss by evapotranspiration, as well as biological activity, which may drive the reaction in the opposite direction (Kämpf and Curi, 2012).

Carbonates occurred in P1 from the surface to the 4Bcḱ horizon, as shown by strong effervescence with 10 % HCl. In P2 and P4, effervescence was very strong in all the horizons, and in P3, it was very strong in the 2Ccrḱ horizon and absent in the others. Reaction intensity was proportional to the $CaCO_3$ equivalent (Table 2). Effervescence with H_2O_2 (20 %), which indicates the occurrence of Mn oxides, was light in all horizons of P1, except for the 5Bvk horizon, and strong in P2, from the Ap1 to Ccmḱ horizon, and in all the horizons of P3 and P4. The results of effervescence with HCl and H_2O_2 did not match, except for the 5Bvk horizon of P1, where both types of effervescence were absent.

Sand, silt, and clay mineralogy by XRD

Sand and silt mineralogy (XRD not shown) in the coarse sand fraction revealed quartz (peaks at 0.426, 0.334, and 0.181 nm) and calcite (0.301, 0.191, 0.187 nm/ 0.382, 0.302, 0.248, 0.227 nm). Small amounts of feldspars were identified in all horizons (peaks at 0.35-0.30 nm/ 0.41, 0.39, 0.33, 0.37 nm/ 0.31 nm/ 0.63-0.65 nm) (Moore and Reynolds Jr, 1989; Oliveira et al., 2004). In the sand fraction of soils from the

Apodi Plateau, Mota et al. (2007) found quartz, goethite, hematite, and magnetite. In a *Cambissolo Háplico* (Inceptisol), Moreira et al. (2000) detected quartz, orthoclase, pyroxene, ilmenite, and small amounts of kaolinite, hematite, and goethite. Calcite was not found in these two studies. However, Lemos et al. (1997) observed quartz, feldspars, and calcite in soils from calcareous material.

The 2Biḱ-P1, Bcmḱ-P2, and Bcḱ-P2 horizons contained traces of Fe oxides or Fe oxide coatings on sand grains. In addition, ferruginous concretions were spread throughout P2. According to Alencar (2002), the reddish colors of soils on the Apodi Plateau are due to quartz and ferruginous concretions in sand fractions, and quartz, mica, and goethite/hematite in the silt fraction.

Fine sand mineralogy was reasonably uniform, characterized mainly by acute and intense peaks of quartz in all the horizons. Calcite was also identified in the horizons with remnants of the carbonate from the parent material (subscript k), along with accumulation of secondary Ca carbonate (subscript ḱ), except for the 5Bvk horizon in P1 and the C horizon in P4. The coarse sand fraction showed small amounts of feldspars. The mineralogy of the sand fraction of three soils with a mollic epipedon in Galicia, Spain, consisted of quartz and feldspars, in addition to mica, goethite, magnetite, and hematite (Taboada Castro and Silva Hermo, 1999). According to the authors, the inheritance of Fe oxides is common in limestone-derived soils.

Silt mineralogy was similar to that of the sand fraction, but showed higher calcite peaks in most horizons. Mica was found in the 2Ccrk-P3 and C-P4 horizons, probably in the form of muscovite (peaks of 0.33, 0.50, and 1.0 nm). Micaceous minerals are common in calcareous materials (Kämpf and Curi, 2003), and the basal asymmetry, along with the larger width at half height (WHH), suggests that they underwent partial weathering (Oliveira et al., 2004). In India, Shankar and Achyuthan (2007) observed a change in the mineralogy of calcareous soil with depth and reported chlorite, quartz, hornblende, garnet, hematite, calcite, and feldspar in the coarse sand fraction.

The frequent occurrence of calcite in sand and silt fractions in the Apodi Plateau originates from the dry climate, which favors the accumulation of secondary calcium carbonate in the soil, and calcite is also inherited from carbonates from the parent material. Quartz is an accessory mineral in limestone, and quartz levels depend on rock purity. The mineralogy reported here is in accordance with that described by West et al. (1988) for limestone-derived soils in central Texas (USA), and by Lemos et al. (1997), Alencar (2002), and Ernesto Sobrinho (1979) for soils on the Apodi Plateau.

Smectite was found in the clay fraction of P1 (Figure 2) and some horizons of P2 (Ccmḱ and Crk) and P3 (2Crk). Smectite peaks were detected at 1.4-1.5 nm, indicated by the patterns of Mg saturated samples when the mineral expanded to 1.7-1.8 nm after solvation with ethylene-glycol, contracted to 1.2 nm when K saturated, and then contracted to 1.0 nm when heated to 550 °C. Smectite in the soil is either inherited from the parent material or derived from lithologic discontinuity, that is, variations in the sediments. In Northeastern Brazil, the occurrence and persistence of smectite in soils is associated with a dry climate and limited water supply, which prevents desilication (Corrêa et al., 2003).

Illite was identified in the C-P4, Bt2c-P3, and Bcmk horizons of P2 (peaks at 1.0, 0.501, and 0.334 nm). Interstratified illite-smectite (Il-Vm) was identified in the P1 profile and in some horizons of P2 (Ccmḱ and Ccrk) and P3 (2Ccrk), and Il-Vm peaks intensified after solvation and heating treatments. Most horizons studied in P2 (Biḱ, Bicḱ, and Bcmḱ) (Figure 3), the Bt2c horizon in P3 (Figure 4), and the C horizon in P4 (Figure 5) exhibited Il-Vm in the clay fraction, with asymmetric peaks from 1.0 to 1.214 nm after heating to 550 °C (Douglas, 1989). In profiles P2 and P3, the patterns observed in the C layer were different from those described above because they exhibited Il-Vm in the surface horizons and smectite/illite-smectite in the deepest layers.

Kaolinite was the main clay mineral in all the horizons in P2, P3, and P4 (Figures 3, 4, and 5). The characteristic peaks were detected at 0.72 and 0.35 nm, disappearing after heating to 550 °C. The peaks were intense, and the small WHH from surface to the deepest horizons suggests good crystallinity of kaolinite.

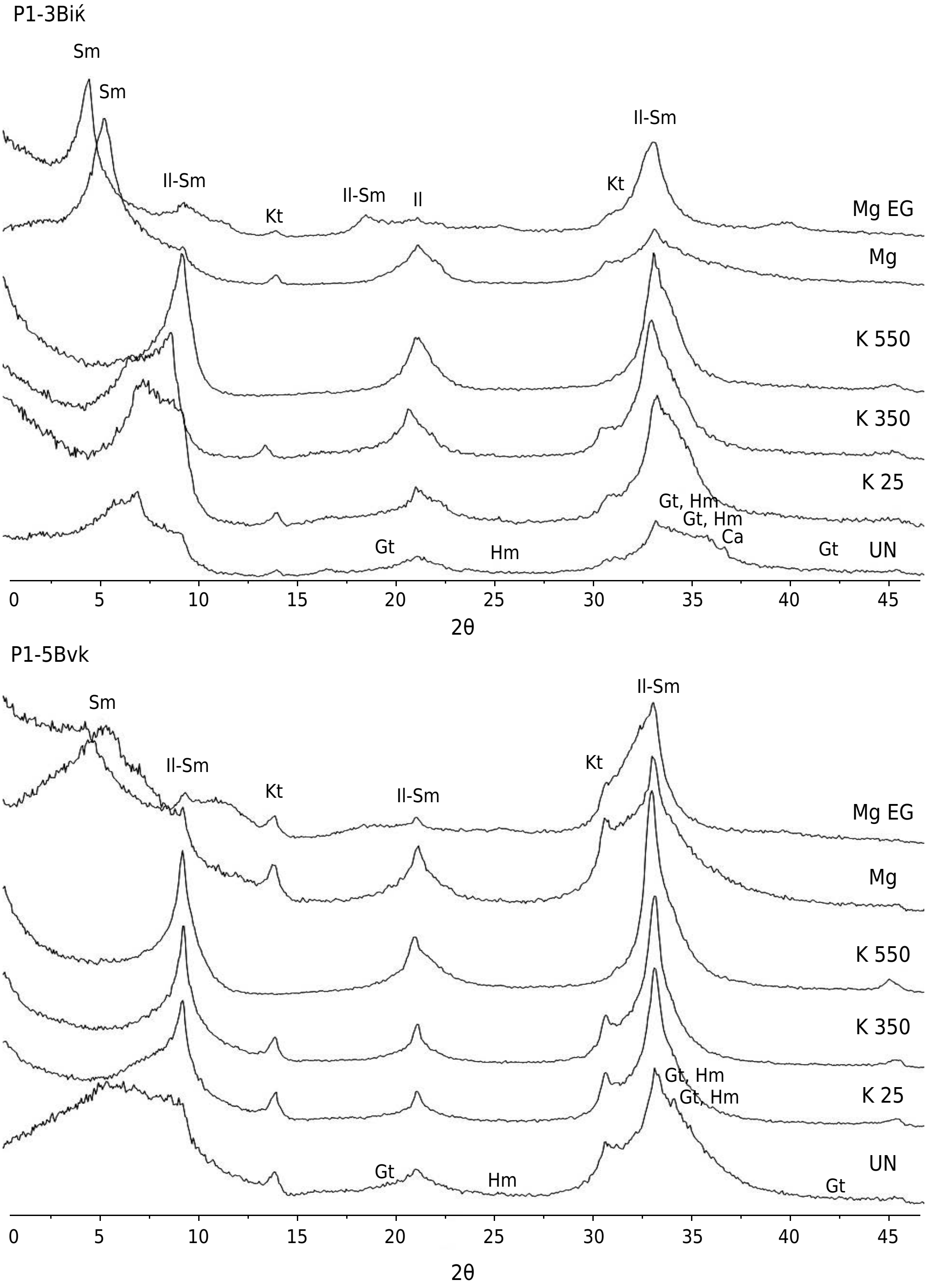

Figure 2. Diffractograms of the clay fraction of soil profile 1 (P1), 3Biḱ and 5Bvk horizons. Calcite (Ca), Smectite (Sm), Illite (Il), Kaolinite (Kt), Goethite (Gt), Hematite (Hm), Untreated total sample (UN), iron-free sample saturated with magnesium (Mg) and solvated with magnesium and ethylene-glycol (MgEG), iron-free sample saturated with potassium at room temperature (K25), and after heating at 350 °C (K350)and 550 °C (K550).

The Fe oxides hematite (peaks at 0.367, 0.266, 0.249, 0.245, and 0.219 nm) and goethite (peaks at 0.418, 0.269, 0.249, 0.245, and 0.219 nm), most common in tropical soils, were also found in the clay fraction of all horizons. High temperatures favor hematite formation, while low pH, high moisture, and high soil organic C content favor goethite (Kämpf and Curi, 2003). Calcite was identified in all horizons of P1 (except for 5Bvk), P2, and P4, with a characteristic peak at 0.301nm. All horizons in P2 (except for Cckr), P3, and P4 contained anatase, identified by a peak at 0.352 nm after elimination of the kaolinite peak by heating.

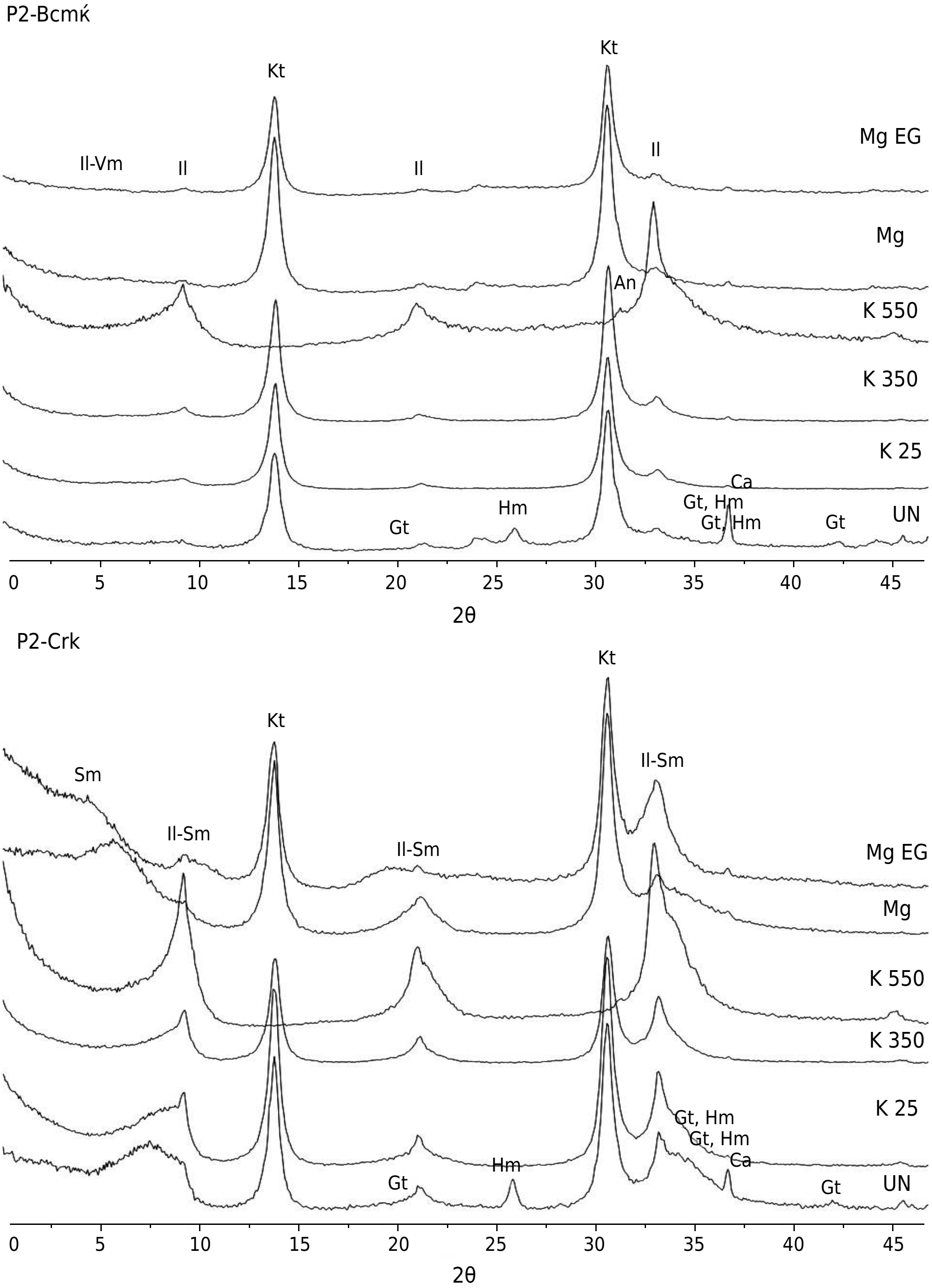

Figure 3. Diffractograms of the clay fraction of soil profile 2 (P2), Bcmḱ and Crk horizons. Calcite (Ca), Smectite (Sm), Illite (Il), Kaolinite (Kt), Goethite (Gt), Hematite (Hm), Vermiculite (Vm), Anatase (An). Untreated total sample (UN), iron-free sample saturated with magnesium (Mg) and solvated with magnesium and ethylene-glycol (MgEG), iron-free sample saturated with potassium at room temperature (K25), and after heating at 350 °C (K350) and 550 °C (K550).

Other studies report that kaolinite, vermiculite, smectite, illite, and chlorite are found in the clay fraction of soils in semi-arid climates and limestone-derived soils (Ernesto Sobrinho, 1979; West et al., 1988; Lemos et al., 1997; Oliveira et al., 1998; Alencar, 2002; Khormali et al., 2003; Mota et al., 2007; Shankar and Achyuthan, 2007; Emadi et al., 2008). Palygorskita was also reported in these soils (Emadi et al., 2008).

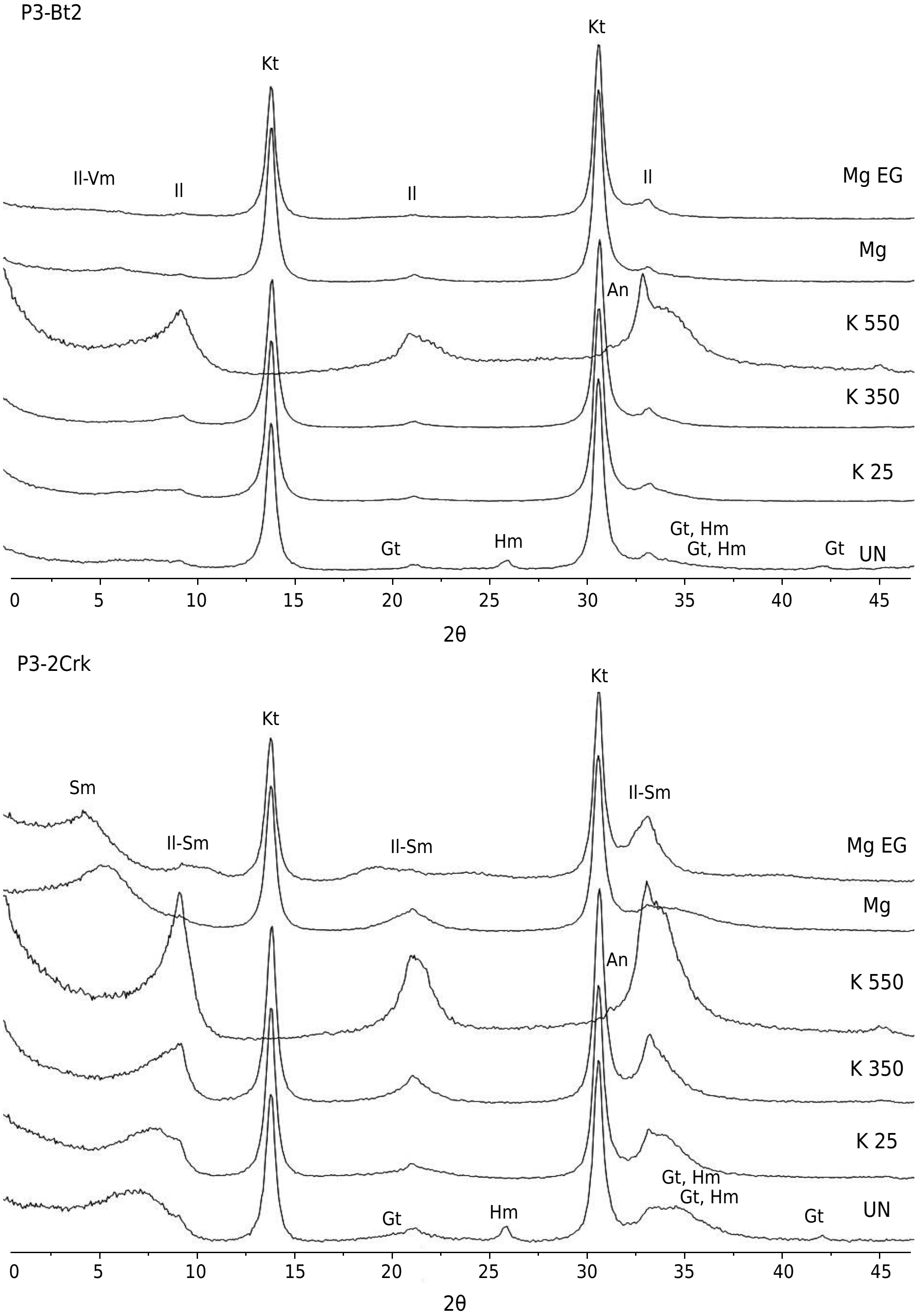

Figure 4. Diffractograms of the clay fraction of soil profile 3 (P3), Bt2 and P3-2Crk horizons. Smectite (Sm), Illite (Il), Kaolinite (Kt), Goethite (Gt), Hematite (Hm), Vermiculite (Vm), Anatase (An).Untreated total sample (UN), iron-free sample saturated with magnesium (Mg) and solvated with magnesium and ethylene-glycol (MgEG), iron-free sample saturated with potassium at room temperature (K25), and after heating at 350 °C (K350) and 550 °C (K550).

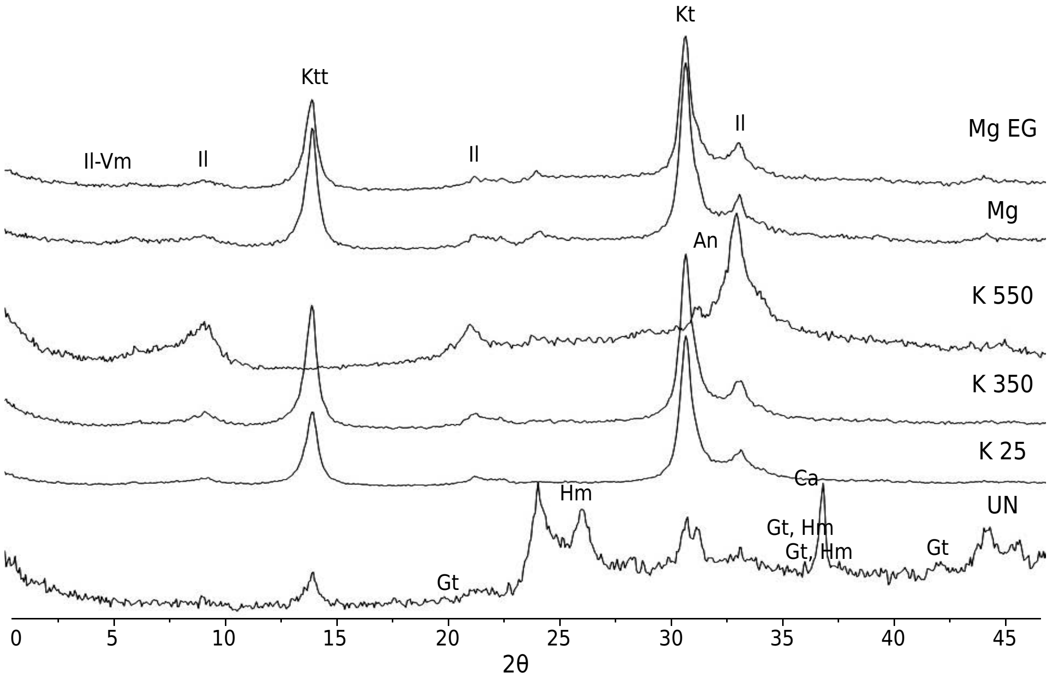

Figure 5. Diffractograms of the clay fraction of soil horizons in profile 4 (P4). Illite (Il), Kaolinite (Kt), Goethite (Gt), Vermiculite (Vm), Anatase (An). Untreated total sample (UN), iron-free sample saturated with magnesium (Mg) and solvated with magnesium and ethylene-glycol (MgEG), iron free sample saturated with potassium at room temperature (K25), and after heating at 350 °C (K350) and 550 °C (K550).

Micromorphology

Micromorphological examination of samples from selected horizons in P1 and P2 (Table 4) revealed strong particle aggregation and well-developed microstructure, with predominance of blocks. The blocky structure was also described in the field observations, although the degree of development was reported as weak to moderate.

In P1, the thin section of the 3Biḱ horizon (Figure 6) showed a heterogeneous matrix with small zones of dense material (20 %) composed of finer particles than those in the surrounding areas. The coarse material corresponding to the sand fraction was primarily composed of well-selected quartz and feldspar minerals that were rounded and sub-angular (anhedral), with a linear alteration pattern and corrosion features. These characteristics suggest that P1 is of colluvial origin. The fine material (fabric) consisted primarily of clay and iron oxides (Figure 6, P1-3Biḱ), which gave a dark yellow-brownish color to the fabric background.

On both slides examined, the orientation was stipple-speckled and striated b-fabric [granostriated and porostriated (Figure 6, Table 4)]. This pattern is produced by the presence of expansive clays, which cause compression and expansion between aggregates and the fabric. The material also features crystallitic b-fabric, characterized by the presence of calcite microcrystals associated with clays, as was indicated by their birefringence (Bullock et al., 1985), especially in the Bicḱ horizon of P2 (Figure 6), which contained high carbonate levels. The association of clay and carbonate in a same horizon provides evidence of a polygenic development (Chadwick et al., 1995).

The complex microstructure was associated with sub-angular and granular blocky aggregate types that account for matrix heterogeneity. The dominance of chambers over other pore types (Table 4) may be associated with the expansion capacity of the material. Artifact-like fractured pores were formed because calcareous soils are difficult to impregnate, due to expansive clays; for quantification of pores, they should be separated to avoid overestimation of porosity.

In P1 and P2, the crystalline pore coating and filling with calcite (Rvc and Prc, respectively, Figure 6) indicated crystallization in the pores, likely caused by ion migration through the soil solution. This process is common in soils from semi-arid climates because of the long dry periods they undergo, which increase solute concentration with salts (Bullock et al., 1985; Castro et al., 2003).

In the Bicḱ horizon of P2, calcite nodules (Ndc) were grayish under natural light and dense, with well-defined limits (Figure 6). Several nodules were coated with Fe oxides and a few were fragmented, possibly because of weathering. The pedogenic origin of carbonates is reinforced by the presence of micrite on nodule edges and pores, possibly formed by primary carbonate dissolution, increased carbonate levels in the soil solution, and precipitation of Ca carbonates in the form of microcrystalline calcite. In addition to the calcite nodules, pure or strongly impregnated nodules were also observed in the horizon. The nodules were possibly composed of Fe and Mn oxides and organic matter, exhibiting a dark brown color, ellipsoidal shape, a smooth surface, and a strong, clear contrast with the matrix background (Figure 6, Table 4). The nodules were at different degrees of decomposition, mainly in the early stages, and some were intact. Calcite nodules were more degraded than iron nodules (Nd), and could be clearly visualized.

In the 3Biḱ horizon of P1, iron coatings and clays were commonly found in soil particles, aggregates, pores, and even in nodules, and Fe hypo-coating (Hp) was observed around the pores (Po) (Figure 6, Table 4). These features are related to the alternation between dry and rainy seasons, which favors clay illuviation, that is, clay removal from the surface and accumulation in subsurface horizons. During illuviation, after soil water evaporates or is absorbed by plants, the clay suspensions in the wetting front are trapped on the surface of the structural units of pore walls. In addition, the pore surface can undergo iron reduction in the rainy season, followed by re-oxidation in the dry season, producing hypo-coatings. The 3Biḱ-P1 slide showed rare excrements, still intact and dense, filling the cavities and resulting in an ellipsoidal and spherical shape. This feature, along with the presence of roots, reveals the existence of biological activity in this horizon.

The matrix in the Bicḱ horizon of P2 was more homogeneous than that of the 3Biḱ horizon of P1 (Figure 6). The coarse fraction in Bicḱ-P2 was primarily composed of quartz (Qz), but the particles were larger and less selected, with a smooth surface, sub-spherical, sub-rounded, and sub-angular shape, intact, and with an irregular linear alteration pattern (Table 4). The fine material content, represented by the clay fraction, was higher than in P1, producing less porosity. The color of the matrix was yellow-brown, likely because of goethite association with calcite. The microstructure of the Bicḱ-P2 was complex, mainly formed by angular and sub-angular blocks and a number of granular blocks (Table 4). The pores (Po) were mostly chambers, followed by fissures, cavities, and, to a lesser extent, channels, suggesting lower biological activity, which is confirmed by the lack of excrements in the sample.

Bicḱ-P2 showed typical carbonate coatings on pores, aggregates, and nodules (Figure 6, Table 4), exhibiting crystallinity. The horizon also contained pores filled with discontinuous loose carbonate material and with continuous loose adherent material, with a similar composition to that of the soil matrix. Iron coatings or hypo-coatings were not observed. Calcite nodules (Ndc) were more abundant and larger than in 3Biḱ-P1, exhibiting typical, concentric, and pure nodules, strongly impregnated by carbonate materials and exhibiting a clear limit with the soil matrix.

The pedogenic origin of Ca carbonate in the 3Biḱ horizon of P1 was confirmed by the crystallinity of the coatings and the frequent micrite fillings. Loose and discontinuous fillings in the micritic nodules commonly observed in Bicḱ-P2 were likewise crystalline. The absence of calcite suggests that the site is a non-calcified zone or has not undergone recent decalcification (Khormali et al., 2003). The calcite nodules identified in calcic horizons by Shankar and Achyuthan (2007) were quartz grains cemented by micrite. Khormali et al. (2003) also observed several calcite features in Iranian soils.

Calcite coatings and Fe coatings or quasi-coatings were found in the 3Biḱ horizon of P1 (Figure 6). They were associated with illuviation of fine particles and Fe oxides, which accumulated along channels and empty spaces in the subsurface. Calcium carbonate coating by clay films is a process associated with climate changes between rainy and dry seasons (Khormali et al., 2003). Similar coatings were reported by Khormali et al. (2003), and the

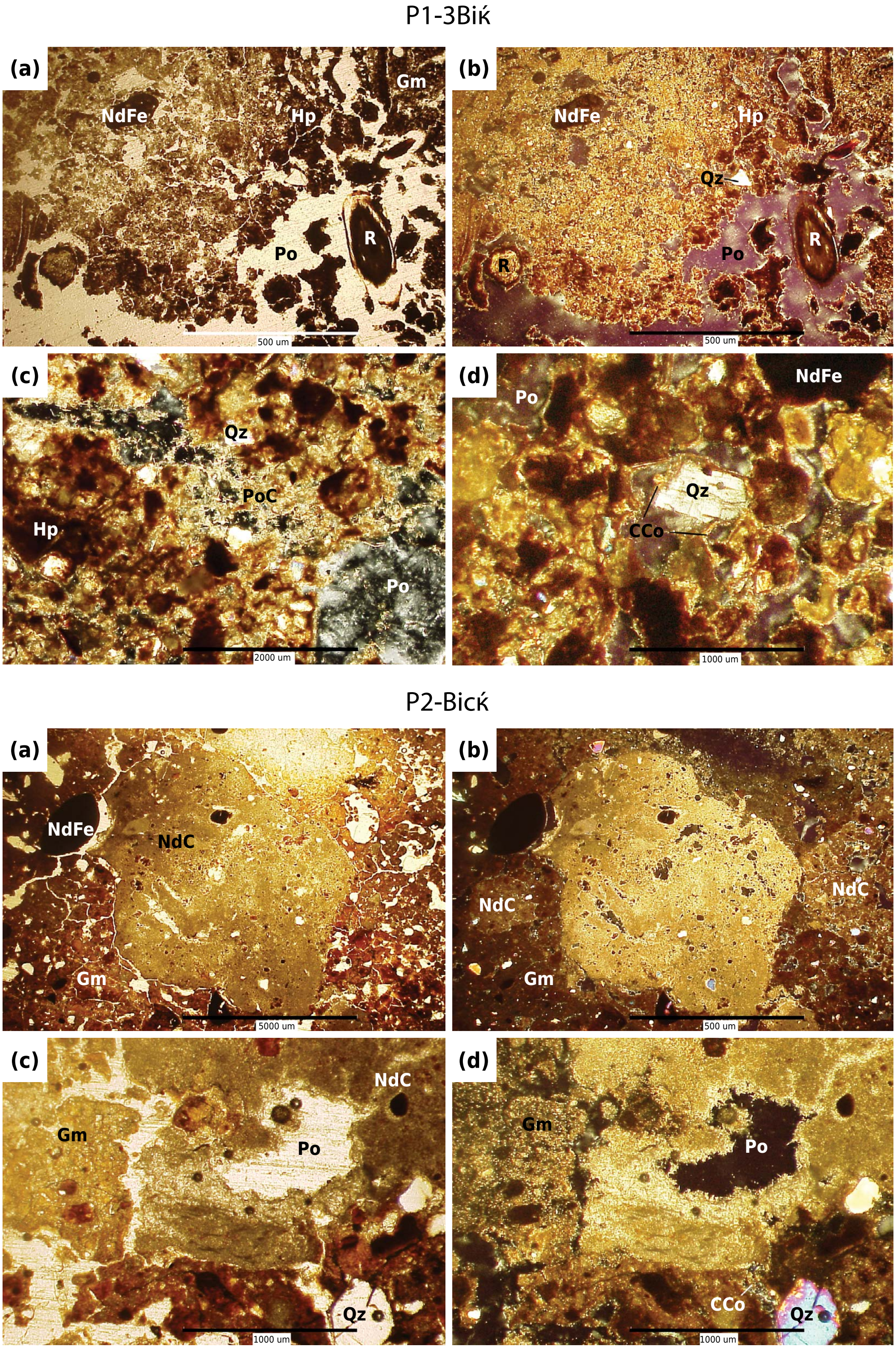

Figure 6. Micropedological features of the P1-3Biḱ and P2-Bicḱ horizons distributed in the matrix and observed under natural (a) and polarized light (b, c, d). Quartz (Qz), Pores (Po), Iron nodules (NdFe), Iron hypo-coating (Hp), Traces of root tissues (R), Calcite nodules (NdC), matrix with birefringent crystals (Gm), Calcite coating (CCo), Calcite-filled pore (PoC).

authors explained their origin by post-recalcification and carbonate movement throughout the profile. Gile et al. (1966) state that illuviation features of clay were first formed in wet climate conditions and subsequently covered over by features of Ca carbonate concentration in the dry season. Chadwick et al. (1995) concluded that pedogenic processes occurring under climatic extremes lead to the development of soils with polygenetic features.

Pedogenesis, soil classification, and contribution to the SiBCS

The pedogenesis of the soils sampled along the transect on the Apodi Plateau was affected by climate, surface relief, and parent material stratification, producing sites or varied degrees of development of soils from the Jandaira Formation (P2, P3, and P4) and derived sediments (P1). The development stages identified were represented by an incipient B horizon in P1 and P2, and a textural (argillic) B horizon in P3. No diagnostic subsurface horizon was found in P4. Therefore, the degree of pedogenic development follows the order P3>P2>P1>P4.

The location of P1 on the footslope promoted high water infiltration and input of soluble bases that were carried from the upslope area, as indicated by the high Ca^{2+} and $CaCO_3$ levels. The parent material was sediment reworked from limestone of the Jandaira Formation, resulting in a lithologic discontinuity represented in the identification of horizons. From the Bcmḱ horizon to deeper layers of P2, the accumulation of calcium carbonates, including petroplinthite, suggests the occurrence of recalcification at depth (the "c" suffix indicates the occurrence of gravel in the Ccmḱ horizon, found at 0.79-0.86 m). However, in Bicḱ-P2, at a depth of 0.32-0.51 m, the loose and discontinuous fillings of micrite nodules suggest the process of decalcification. This feature is probably caused by the current climate changes in the region, that is, the higher frequency of intense rainfall events of shorter duration, resulting in dissolution of the carbonate accumulated in the soil.

Profile P3 exhibited the highest degree of pedogenic development, despite being surrounded by a soil profile (P2) with incipient development, under similar plain topography, semi-arid climate, chronology of geological formation, and vegetation (hyper-xerophytic *caatinga*). The mineralogical profile of the silt fraction (with calcite occurrence) and clay minerals of P3 was similar to that of P2, and the alkalinity of both profiles may be related to influence of the calcareous lithology. In P4, the rolling topography and backslope location favored exportation of materials. Thus, P4 soil developed directly from the rock, and it exhibits little pedogenic evolution.

The most intense pedogenic processes were: a) argilli pedoturbation in the 5Bvk-P1 horizon (0.56-0.95 m), indicated by the v suffix (vertic character), and characterized by the large prismatic structures and extremely hard and firm soil consistency; b) elluviation/illuviation in P3, with clay accumulation (suffix Bt); and c) calcification, identified by $CaCO_3$ accumulation (ḱ), and plinthite formation (c suffix) in P2 and P3.

According to current criteria established by the SiBCS, the classification of the soils is: P1 – *Cambissolo Háplico Carbonático vertissólico*, P3 – *Luvissolo Crômico Palico petroplíntico,* and P4 – *Neossolo Litólico Carbonático típico*. In addition, because of the large $CaCO_3$ content in P4 (472.0 g kg^{-1}), we recommend that an additional class of hyper carbonate should be used to differentiate this profile in the fifth level of the Brazilian soil classification system.

Up to this time, there is not a thorough report on petrocalcic horizons occurring in Brazilian soils with a detailed characterization of their genesis, micromorphology, and mineralogy. The morphology of Bcmḱ-P2 showed strong cementation, thickness of more than 0.10 m, and a large amount of $CaCO_3$ equivalent. However, because it is discontinuous, it does not fulfill all the requirements determined by the SiBCS (Santos et al., 2013) for petrocalcic horizons. Given the partial cementation of P2 horizons by carbonates, the application of the term *parapetrocalcic* in the fourth level of the SiBCS is suggested, since the lack of continuity diverge from a petrocalcic horizon. In addition, given that the amount of petroplinthite in deep horizons is not sufficient to meet *Plintossolos* requirements, it is proposed that P2 should be classified as of the concretionary subgroup instead of the typic (*Cambissolo Háplico Carbonático concrecionário* instead of *Cambissolo Háplico Carbonático típico*).

The morphological, chemical, mineralogical, and micromorphological features described, support the hypothesis of alternating episodes of sedimentation and climatic oscillation in the study area. The main evidences are: coexistence of carbonate and petroplinthite in the profile; calcite and Fe coating and quasi-coating associated with illuviation of fine particles and Fe oxides, with accumulation in subsurface layers; contrasting pedogenic mineral phases (kaolinite, smectite, illite-smectite, illite-vermiculite) in the profiles; and variation in particle size. Morrison (1967) adopted the concept of polygeny to indicate polygenic profiles, that is, soils formed because of the overlapping of different pedogenic evolution phases. The application of this concept is therefore suitable for the pedogenesis of soils on the Apodi Plateau.

CONCLUSIONS

The soil chemical and morphological properties, associated with profile position in the landscape, suggest a strong influence of the calcareous parent material and associated sediments in soil formation. However, the irregular distribution of $CaCO_3$ in the profile; the soil mineralogy with predominance of kaolinite, interstratified minerals, and smectite; and the micromorphological features associated with micrite suggest that paleoclimate and poligeny affected the pedogenesis.

Based on the evaluated soil properties, including mineralogical and micromorphological features, the evolutionary sequence (from more to less developed) of the profiles of the Apodi Plateau is P3>P2>P1>P4.

Given the discontinuous calcium carbonate cementation in P2 and high frequency of petroplinthite nodules and concretions, the classification as *Cambissolo Háplico Carbonático parapetrocálcico concrecionário* in the fourth level of the SiBCS is proposed.

ACKNOWLEDGMENTS

Our thanks to CPGA-CS and UFRRJ, the UFC, and the CNPq (Edital MCT/ CNPq 14/2009) for financial support and supervision. To Embrapa Solos and the Laboratories of Mineralogy and Micromorphology of Soils of ESALQ/USP for technical support.

REFERENCES

Alencar ELL. Química e mineralogia de três pedons originários de calcário da Chapada do Apodi – CE [dissertação]. Fortaleza: Universidade Federal do Ceará; 2002.

Bachman GO, Machette MN. Calcic soils and calcretes in the southwestern United States. United States of America, U.S. Geol Survey (USGS). 1977:77-797. doi:10.1016/j.geoderma.2015

Brasil. Ministério da Agricultura. Levantamento exploratório – reconhecimento de solos do Estado do Ceará. Recife: 1973. v.1.

Brasil. Ministério das Minas e Energia. DNPH. Projeto RADAMBRASIL: folha SB.24/25 Jaguaribe/Natal: geologia, geomorfologia, pedologia, vegetação e uso potencial da terra. Rio de Janeiro: 1981. (Levantamento dos recursos naturais, 23).

Bullock P, Fedoroff N, Jongerius A, Stoops G, Tursina T. Handbook for soil thin section description. London: Waine Research Publications; 1985.

Castro SS, Cooper M, Santos MC, Vidal-Torrado P. Micromorfologia do solo: bases e aplicações. Tópicos Cienc Solo. 2003; 3:107-64.

Chadwick OA, Nettleton WD, Staidl GJ. Soil polygenesis as a function of quaternary climate change, Northern Great Basin, U.S.A. Geoderma. 1995;68:1-26. doi:10.1016/0016-7061(95)00025-J

Claessen MEC, organizador. Manual de métodos de análise de solo. 2ª ed. Rio de Janeiro: Centro Nacional de Pesquisa de Solos; 1997.

Corrêa MM, Ker JC, Mendonça ES, Ruiz HA, Bastos, RS. Atributos físicos, químicos e mineralógicos de solos da região das várzeas de Sousa (PB). Rev Bras Cienc Solo. 2003;27:311-24. doi:10.1590/S0100-06832003000200011

Dal'Bó PFF, Basilici G. Estimativas de paleoprecipitação e gênese de feições cálcicas e argílicas em paleossolos da Formação Marília (Neocretáceo da Bacia Bauru). Geociências. 2010;29:33-47.

Douglas LA. Vermiculites. In: Dixon JB, Weed SB, editors. Minerals in soil environments. Madison: Soil Science Society of America; 1989. p.635-74.

Emadi M, Baghernejad M, Mermarian H, Saffari M, Fath H. Genesis and clay mineralogical investigation of highly calcareous soils in semi-arid regions of Southern Iran. J Appl Sci. 2008;8:288-94. doi:10.3923/jas.2008.288.294

Ernesto Sobrinho F. Caracterização, gênese e interpretação para uso de solos derivados de calcário da região da Chapada do Apodi, Rio Grande do Norte [dissertação]. Viçosa, MG: Universidade Federal de Viçosa; 1979.

Fernandes MAB, Santiago MMF, Gomes DF, Mendes Filho J, Frischkorn H, Lima JOG. A origem dos cloretos nas águas subterrâneas na Chapada do Apodi-Ceará. Águas Subterrâneas. 2005;9:25-34. doi:10.14295/ras.v19i1.1349

Gile LH, Peterson FF, Grossman, RB. Morphological and genetic sequences of carbonate accumulation in desert soils. Soil Sci. 1966;101:347-54. doi:10.1097/00010694-196605000-00001

Girão RO. Pedogênese em um ambiente cárstico no clima semiárido em Limoeiro do Norte – Ceará [dissertação]. Fortaleza: Universidade Federal do Ceará; 2011.

Hendricks DM. Genesis and classification of arid region soils. In: Skujins J, editor. Semiarid lands and deserts: soil resource and reclamation. New York: Marcel Dekker; 1991. p.33-80.

Holliday VT. Morphology of late Holocene soils at the Lubbock Lake archeological site, Texas. Soil Sci Soc Am J. 1985;49:938-46. doi:10.2136/sssaj1985.03615995004900040030x

Kämpf N, Curi N. Argilominerais em solos brasileiros. Tópicos Cienc Solo. 2003;3:1-54.

Kämpf N, Curi N. Formação e evolução do solo (pedogênese). In: Ker JC, Curi N, Schaefer CEGR, Vidal-Torrado P, editores. Pedologia: fundamentos. Viçosa, MG: Sociedade Brasileira de Ciência do Solo; 2012. p.207-302.

Khormali F, Abtahi A, Mahmoodi S, Stoops G. Argillic horizon development in calcareous soils of arid and semiarid regions of southern Iran. Catena. 2003;53:273-301. doi:10.1016/S0341-8162(03)00040-7

Khresat SA. Calcic horizon distribution and soil classification in selected soils of north-western Jordan. J Arid Environ. 2001;47:145-52. doi:10.1006/jare.2000.0712

Khresat SA, Taimeh AY. Properties and characterization of Vertisols developed on limestone in a semi-arid environment. J Arid Environ. 1998;40:235-44. doi:10.1006/jare.1998.0445

Lemos MSS, Curi N, Marques JJGSM, Ernesto Sobrinho F. Evaluation of characteristics of Cambisols derived from limestone in low tablelands in northeastern Brazil: implications for management. Pesq Agropec Bras. 1997;32:825-34.

Lynch LS. Gênese e geoquímica de solos em ambiente cárstico no cerrado da região de Planaltina de Goiás [tese]. Viçosa, MG: Universidade Federal de Viçosa; 2009.

Mehra OP, Jackson ML. Iron oxide removal from soil and clays by dithionite – citrate system buffered with sodium bicarbonate. Clays Clay Miner. 1960;5:317-27. doi:10.1346/ccmn.1958.0070122

Moore DM, Reynolds Jr RC. X-ray diffraction and the identification and analysis of clay minerals. Oxford: Oxford University Press; 1989.

Moreira A, Franchini JC, Moraes LAC, Malavolta E. Disponibilidade de nutrientes em Vertissolo calcário. Pesq Agropec Bras. 2000;35:2107-13. doi:10.1590/S0100-204X2000001000024

Morrison RB. Principles of quaternary soil stratigraphy. In: Morrison RB, Wright Jr HE, editors. Proceedings of the 7th Congress Quaternary Soils. Stephenville: Eryops/International Union for Quaternary Research; 1967. v.9. p.1-69.

Mota JCA, Assis Júnior RN, Amaro Filho J, Romero RE, Mota FOB, Libardi P.L. Atributos mineralógicos de três solos explorados com a cultura do melão na Chapada do Apodi – RN. Rev Bras Cienc Solo. 2007;31:445-54. doi:10.1590/S0100-06832007000300004

Oliveira CV, Ker JC, Curi N, Duarte MN, Fontes LE. Caracterização de concreções ferromanganosas de solos de calcário no norte do Estado de Minas Gerais. Rev Bras Cienc Solo. 2001;25:565-74. doi:10.1590/S0100-06832001000300005

Oliveira DP, Ferreira TO, Romero RE, Farias PRS, Costa MCG. Microrrelevo e a distribuição de frações granulométricas em Cambissolos de origem calcária. Rev Cienc Agron. 2013;44:676-84.

Oliveira CV, Ker JC, Fontes LEF, Curi N, Pinheiro, J.C. Química e mineralogia de solos derivados de rochas do Grupo Bambuí no norte de Minas Gerais. Rev Bras Cienc Solo. 1998;22:583-93. doi:10.1590/S0100-06831998000400003

Oliveira LB, Ribeiro MR, Ferraz FB, Ferreira MGVX, Mermut AR. Mineralogia, micromorfologia e gênese de solos planossólicos do sertão do Araripe, Estado de Pernambuco. Rev Bras Cienc Solo. 2004;28:665-78. doi:10.1590/S0100-06832004000400009

Olsen SR, Cole CV, Watanabe FS, Dean LA. Estimation of available phosphorus in soils extraction with sodium bicarbonate. Washington, DC: USDA; 1954. (Circular, 939).

Pansu M, Gautheyrou J. Handbook of soils analysis – mineralogical, organic and inorganics methods. New York: Springer; 2006.

Pereira MG, Schiavo JA, Fontana A, Dias Neto AH, Miranda, LPM. Caracterização e classificação de solos em uma topossequência sobre calcário na serra da Bodoquena, MS. Rev Bras Cienc Solo. 2013;37:25-36. doi:10.1590/S0100-06832013000100003

Rabenhorst MC, West LT, Wilding LP. Genesis of calcic and petrocalcic horizons in soils over carbonate rocks. In: Nettleton WD, editor. Occurrence, characteristics and genesis of carbonate, gypsum and silica accumulations in soils. Madison: Soil Science Society of America; 1991. p.61-74. (Special Publication, 26).

Santos RD, Lemos RC, Santos HG, Ker JC, Anjos LHC. Manual de descrição e coleta de solo no campo. 5ª. ed. Viçosa, MG: SBCS/Embrapa Solos; 2005.

Schwertmann U, Taylor RM. Iron oxides. In: Dixon JB, Weed SB, editors. Minerals in soil environments. Madison: Soil Science Society of America; 1989. p.379-438.

Shankar N, Achyuthan H. Genesis of calcic and petrocalcic horizons from Coimbatore, Tamil Nadu: Micromorphology and geochemical studies. Quatern Int. 2007;175:140-54. doi:10.1016/j.quaint.2007.05.017

Shinzato E. O Carste da Área de Proteção Ambiental de Lagoa Santa (MG) e a sua influência na formação dos solos (tese). Campos dos Goytacazes: Universidade Estadual do Norte Fluminense; 1998.

Silva MB, Anjos, LHC, Pereira MG, Schiavo JA, Cooper M, Cavassani RS. Gênese e classificação dos solos de uma topossequência em área de carste na Serra da Bodoquena, MS. Rev Bras Cienc Solo. 2013;37:1464-80. doi:10.1590/S0100-06832013000600004

Stoops G. Guidelines for analysis and description of soil and regolith thin sections. Madison: Soil Science Society of America; 2003.

Taboada Castro MT, Silva Hermo BM. Characterization of soils with mollic horizon formed over limestone in a humid temperate climate (Galicia, NW Spain). Cad Lab Xeolóxico Laxe Coruña. 1999;24:167-75.

West LT, Drees LR, Wilding LP, Rabenhorst MC. Differentiation of pedogenic and lithogenic carbonate forms in Texas. Geoderma. 1988;43:271-87. doi:10.1016/0016-7061(88)90047-X

Yaalon DH. Soils in the Mediterranean region what makes them different? Catena. 1997;28:157-69. doi:10.1016/S0341-8162(96)00035-5